NASA Technical Memorandum 103726
AIAA-90-5240

Experimental Investigation of a Single Flush-Mounted Hypermixing Nozzle

David O. Davis, Warren R. Hingst and A. Robert Porro
Lewis Research Center
Cleveland, Ohio

Prepared for the
Second International Aerospace Planes Conference
sponsored by the the American Institute of Aeronautics and Astronautics
Orlando, Florida, October 29-31, 1990

NASA

EXPERIMENTAL INVESTIGATION OF A SINGLE FLUSH-MOUNTED HYPERMIXING NOZZLE

D.O. Davis*, W.R. Hingst* and A.R. Porro†
NASA Lewis Research Center, Cleveland, Ohio

Abstract

Reported herein are the results of an experimental wind tunnel investigation of a circular supersonic jet (M_j = 3.47) injected at a 10 degree angle into a supersonic freestream. The jet penetrates a boundary layer, which has a thickness approximately the same as the jet nozzle exit diameter. Measurements were made for nominal freestream Mach numbers of 1.6, 2.0, 2.5 and 3.0. Three jet total pressures were run at each freestream Mach number, resulting in twelve separate operating conditions. Mean data accumulated by means of static and total pressure probe instrumentation are presented at two axial stations: seven jet nozzle diameters upstream and 15 jet nozzle diameters downstream from where the centerline of the nozzle intersects the wind tunnel wall. For one condition at each freestream Mach number, the jet air was seeded with a hydrocarbon trace gas and the flow was sampled at the downstream measurement plane to quantify the mean mixing of the two streams. Surface oil flow visualization was also used to investigate the flow interaction. All results are for air-to-air mixing. The measurements indicate the presence of two pairs of contra-rotating vortices. One pair follows the jet trajectory and tends to split the jet into two streams. A smaller pair, rotating in an opposite sense, develops in the near wall region. Reported results include Mach number and volume fraction distributions in the cross plane, as well as jet penetration and mixing efficiency.

Nomenclature

A_v	= area of mixed gas at measurement plane
A_{total}	= area of wind tunnel at measurement plane
D	= nozzle exit diameter (24.2 mm)
h	= jet penetration height
H_{12}	= boundary layer shape factor (δ_1/δ_2)
M	= Mach number
N	= number of moles
$\bar{M}$	= Mach number ratio (M_j/M_∞)
P	= static pressure
P_{eb}	= effective back pressure
P_t	= total pressure
Re	= unit Reynolds number (U_∞/ν)
T_t	= total temperature
$\bar{q}$	= dynamic pressure ratio $(\rho U^2)_j/(\rho U^2)_\infty$
u'	= RMS axial fluctuating velocity component
U	= axial velocity component
v	= volume (mole) fraction
x, y, z	= cartesian coordinate system (Fig. 2)
δ	= boundary layer thickness
δ_1	= displacement thickness
δ_2	= momentum thickness
θ	= injection angle (10°)
λ	= mass flux ratio $(\rho U)_j/(\rho U)_\infty$
μ	= molecular viscosity
ν	= kinematic viscosity (μ/ρ)
ρ	= density

Subscripts

j	= jet condition
∞	= freestream (tunnel) condition
e	= boundary layer edge condition

Introduction

An experimental study is being conducted at NASA Lewis Research Center to determine the effectiveness of various hypermixing nozzle concepts for NASP propulsion applications. A single flush nozzle has been selected as a baseline model to investigate jet penetration and mixing over a range of operating conditions. Results obtained with this nozzle will provide a comparison for future testing of more complicated multi-nozzle configurations (see Fig. 1). These results will also provide a data base for Computational Fluid Dynamics (CFD) code development.

Nozzles with shallow injection angles represent a compromise between the extremes of normal injection and tangential slot injecton. Jets injected normal to a supersonic stream provide good penetration and mixing, but at the expense of large total pressure loss. Tangential slot injection, on the other hand, contributes all of it's momentum to axial thrust, but with no penetration and little mixing. Multiple shallow angle injectors which are ramped and separated by expansion slots utilize oblique shock interaction and streamwise vorticity generation to enhance mixing.[1] A typical injector block of this type is shown in Fig. 1. In order to evaluate the effectiveness of an injector configuration such as this, it is useful to first consider the case of a flush mounted nozzle to determine the effect of jet properties alone on penetration and mixing.

The injection of an underexpanded secondary jet at a non-zero injection angle into a primary supersonic stream is assumed to be a two-stage process.[2,3] The first stage occurs in the region of initial penetration, where the jet is acceler-

* Aerospace Engineer, Internal Fluid Mechnics Division, Member AIAA.

† Aerospace Engineer, Internal Fluid Mechnics Division.

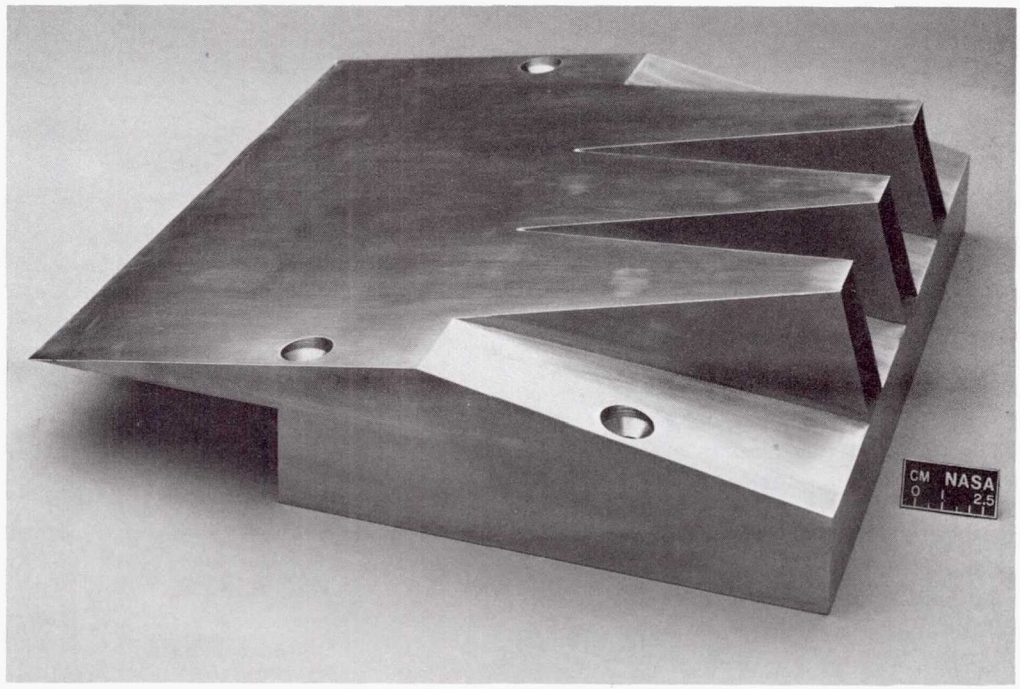

Fig. 1. Swept ramp hypermixing nozzle.

ated and turned in the direction of the primary stream. Little mixing occurs in this region. The second stage is nearly coaxial turbulent mixing of the two streams. The presence of the jet acts as an obstacle to the primary stream and generates an interaction shock that increases the effective back pressure of the jet. The flow expands in the presence of the effective back pressure until a normal shock (Mach disk) occurs. Schetz *et al.*[4] proposed that an analogy exists between injection into a supersonic cross stream and injection into a quiescent medium. By suitable definition of the effective back pressure, the penetration of the Mach disk could be predicted from the well-understood theory of the latter case. Schetz found that for normal injection of a sonic jet[5] and supersonic jet[6] into a supersonic cross stream, the penetration of the Mach disk correlated well when the effective back pressure was defined as 80% of the static pressure behind a normal shock in the freestream. Recently, Mays *et al.*[7] suggested that for shallow angle injection, the effective back pressure could be approximated by assuming that the jet appeared to the freestream as a half cone with a half-angle equal to the injection angle.

Analytic jet penetration models for normal injection[3,5,8] and for angled injection[9–11] have been developed. These models, however, were formulated to predict the penetration of the Mach disk and are restricted to the nearfield interaction region. In the downstream region, the jet decays by turbulent mixing and is distorted by streamwise vortices as illustrated in Fig. 2.[12] Correlations for penetration in the downstream region have been proposed by Orth *et al.*[2] and Faucher *et al.*[13] for normal sonic injection and by McClinton[14] for angled sonic injection of multiple jets. Rogers[15,16] attempted to correlate his normal single and multiple sonic jet data with the model given in Refs. 2 and 13 with limited success. Mays *et al.*[7] found poor agreement between their shallow angle sonic injection and the correlation proposed by McClinton.

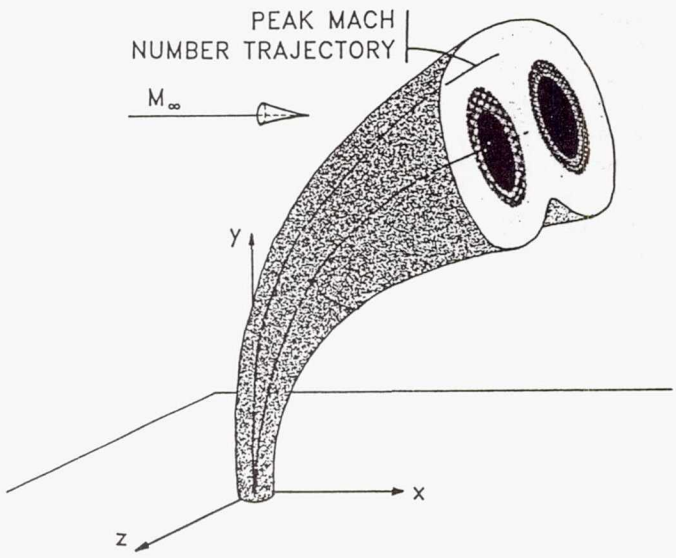

Fig. 2. Sketch of normal jet flowfield.[12]

At present, jet penetration and mixing correlations for shallow angle supersonic injection into a supersonic stream are virtually non-existent due to the lack of experimental data. In addition, detailed data in the transverse plane is required to support CFD code validation and calibration.

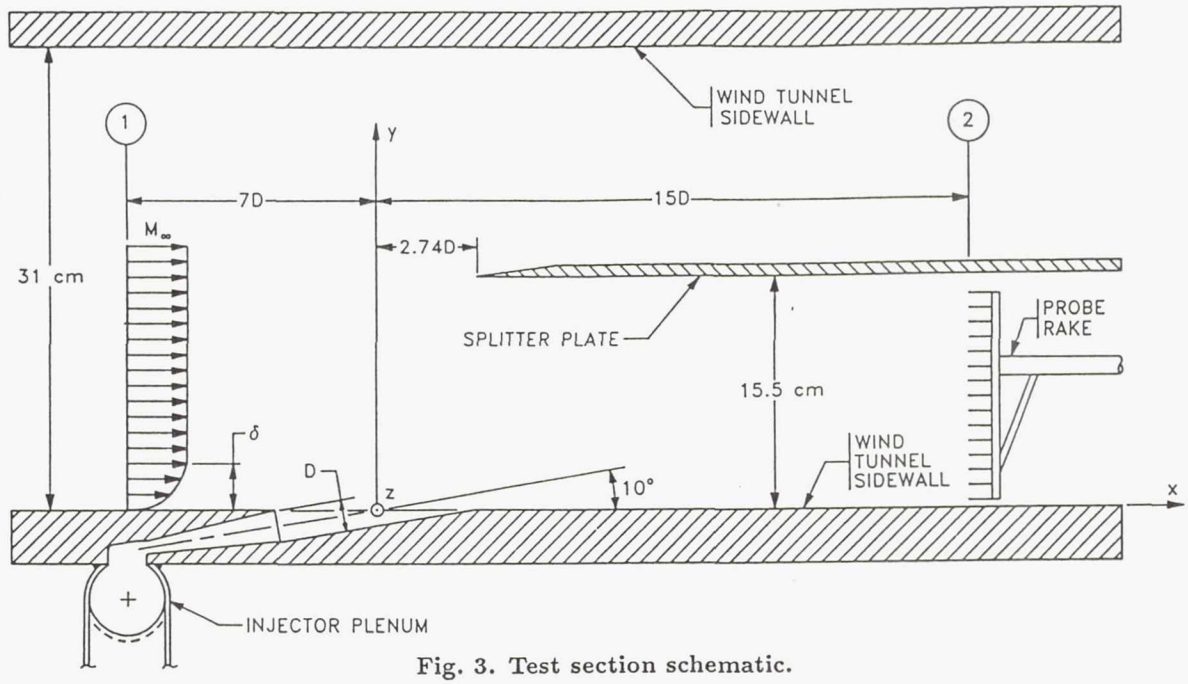

Fig. 3. Test section schematic.

The present study was initiated to help fill this void. The nozzle configuration chosen for this study consists of a circular supersonic jet (M_j=3.47) injected at a 10 degree angle into a supersonic freestream. The jet penetrates a boundary layer whose thickness is approximately the same as the nozzle exit diameter.

Experimental Program

Flow Facility

The flow facility used in this study was the NASA-Lewis Research Center 1×1-foot Supersonic Wind Tunnel. This wind tunnel is a continuous, open-loop flow facility with a Mach number range from 1.3 to 5.5 provided by interchangeable nozzle blocks. A schematic of the wind tunnel test section with the injector nozzle installed is shown in Fig. 3. The nozzle is located halfway across one of the wind tunnel sidewalls whose height is 30.5 cm. A splitter plate, which supports the probe traverse mechanism, is located at the midspan of the wind tunnel. Reference coordinates for this configuration and the two axial locations where data were accumulated are also indicated in Fig. 3.

Pressure Probe Instrumentation

The test section was outfitted with both static and total pressure instrumentation. Static pressure at the upstream station was sampled by means of 0.51 mm diameter wall taps. Boundary layer surveys at the upstream location were measured with a flattened pitot tube having outer dimensions of 0.81 × 0.41 mm at the tip. Static pressure in the cross plane at the downstream station was measured with a 15 tube cone-cylinder probe rake. The half-angle of the cone was 5°, the diameter of each probe was 1.02 mm and the tubes were spaced 9.53 mm apart. Pitot pressure at the downstream station was measured with a 15 tube pitot rake, which had the same nominal dimensions as the static pressure rake. The rakes were positioned such that the probes lay in a plane parallel to the x-y plane.

Trace Gas Instrumentation

A hydrocarbon trace gas technique was used to measure the mean mixing of the two streams. The supply line to the nozzle was seeded with ethylene at a location approximately 60 supply line pipe diameters (Pipe I.D.=5.08 cm) upstream from the injector plenum to ensure thorough mixing. An Edwards Model 825 mass flow controller maintained the ethylene flow at a constant rate. At the downstream measurement plane, the flow was sampled by means of the pitot tube rake described in the previous section. The sampled gas passed through a series of pumps and back pressure regulators before entering a Gow-Mac Model 23-500 total hydrocarbon analyzer. Because the gas route must be completely purged of the previous data point sample before a current reading is taken, the time between readings is relatively long; approximately 30 seconds. In contrast, a pressure measurement typically takes 5-10 seconds. The output of the analyzer is a voltage linearly proportional to the number of carbon atoms flowing through the unit. The analyzer is calibrated with zero gas air and an NBS grade reference mixture of propane and zero gas air (475 ppm). For the two jet total pressures considered for the trace gas measurements, namely; 2.07 and 2.76 MPa, the ethylene concentration in the jet plenum was observed to be 150 and 112 ppm, respectively.

When properly calibrated, the trace gas analyzer displays the volume (mole) fraction of ethylene, which for the present case is equivalent to the mass fraction. Readings taken in the measurement plane, when normalized by the volume fraction in the jet plenum, yield the volume fraction of the jet to tunnel flow:

$$v_j = \frac{(N_{ethylene}/N_{total})}{(N_{ethylene}/N_j)} = \frac{N_j}{N_{total}} \qquad (1)$$

Table 1. Operating Conditions

Case	M_∞	$P_{t,\infty}$ (kPa)	$P_{t,j}/P_{t,\infty}$	P_j/P_∞	P_j/P_{eb}	U_j/U_∞	λ	$\bar{q}$
1	1.6	89.6	15.4	0.86	0.69	1.45	2.83	4.10
2	1.6	89.6	23.1	1.29	1.03	1.45	4.25	6.15
3*	1.6	89.6	30.8	1.72	1.37	1.45	5.67	8.20
4	2.0	137.8	10.0	1.03	0.77	1.26	2.48	3.14
5*	2.0	137.8	15.0	1.54	1.15	1.26	3.73	4.71
6	2.0	137.8	20.0	2.05	1.53	1.26	4.97	6.28
7	2.5	172.4	8.00	1.79	1.21	1.13	3.11	3.51
8*	2.5	172.4	12.0	2.69	1.81	1.13	4.66	5.27
9	2.5	172.4	16.0	3.58	2.42	1.13	6.21	7.03
10	3.0	206.8	6.67	3.21	1.95	1.05	4.16	4.37
11*	3.0	206.8	10.0	4.82	2.93	1.05	6.24	6.55
12	3.0	206.8	13.3	6.42	3.90	1.05	8.32	8.74

M_j=3.47, $T_{t,j}$=$T_{t,\infty}$=294.0 K, θ=10° (all cases)

Results and Discussion

Operating Conditions

Data were accumulated for freestram Mach numbers of 1.6, 2.0, 2.5 and 3.0. At each Mach number, three jet total pressures were considered, resulting in a total of 12 operating conditions. However, due to the long time required to analyze a trace gas sample, trace gas measurements were made at only one condition per Mach number. The 12 operating conditions are summarized in Table 1. Asterisks by the Case number indicate that trace gas measurements were made. The total temperature of the streams was nominally the same (T_t=294° K).

Following Mays *et al.*[7], the effective back pressure (P_{eb}) is defined as the surface pressure on a cone in the freestream which has a half-angle equal to the injection angle. Assuming this to be a valid approximation, then test Cases 1 and 4 are at a overexpanded condition. The pressure ratio for Case 2 is nearly at a matched condition, while the remainder of the cases are at underexpanded conditions.

Disturbances in the freestream generated by the presence of the jet will propagate outward at an angle slightly larger than the Mach angle associated with the freestream condition. These waves will reflect from the wind tunnel walls and pass through the jet stream. This is an important consideration because the interaction between an oblique shock and a mixing layer is known to increase the rate of mixing between the streams[1,17]. The path of these disturbances was estimated for the present configuration. For the two lower freestream Mach numbers, multiple reflections occur before crossing the measurement plane. For the two higher Mach numbers, the waves pass through the measurement plane without crossing the jet stream.

Boundary Layer Profiles

Inasmuch as this study is intended to support concurrent CFD efforts at the NASA Lewis Research Center, it was considered important to provide well documented upstream flow conditions. To this end, boundary layer profiles were measured along the wind tunnel wall bisector at a location seven nozzle diameters upstream from where the nozzle centerline intersects the wall (x=0). Mean velocity profiles for the four freestream operating conditions are plotted in Fig. 4. Previous hot-wire measurements and analysis of the profiles have shown that the boundary layers are fully turbulent. Integral parameters as well as freestream turbulence intensity are summarized in Table. 2.

Table 2. Upstream Flow Condition

M_∞	1.6	2.0	2.5	3.0
δ/D	0.924	1.081	1.265	1.110
δ_1/D	0.175	0.230	0.290	0.347
δ_2/D	0.078	0.083	0.081	0.075
H_{12}	2.240	2.770	3.580	4.630
u'/U_∞ (%)	0.470	0.450	0.380	0.410

D = 24.2 mm

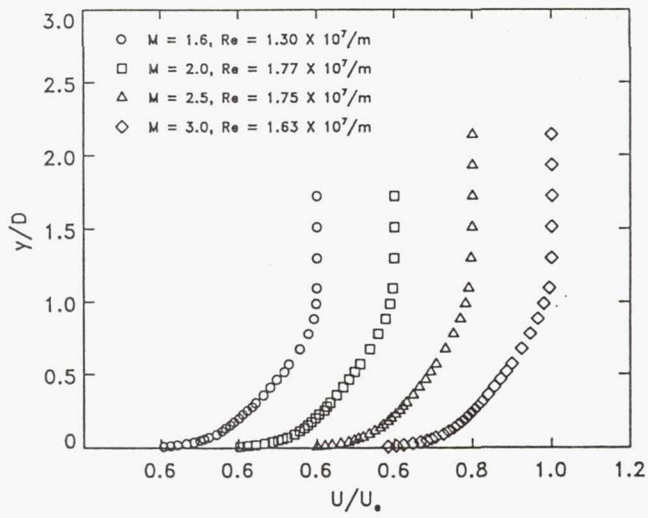

Fig. 4. Mean velocity profiles at x/D=-7.

Flow Visualization

A qualitative assesment of the near wall flow behavior was obtained by means of surface oil flow visualization. The entire wall of the test section was painted with a mixture of SAE 140W oil and a flourescent dye. The oil was brushed on with strokes perpendicular to the primary flow direction. The wind tunnel was run until a steady pattern was established (approximately 15 minutes) and then rapidly shutdown to preserve the flow pattern. An ultraviolet light was used to illuminate the dye pattern. The results for Case 8 are shown in Fig. 5. The results for the other flow conditions exhibited the same general behavior as this case. The flow pattern shows no indication of flow separation, although a small region may exist immediately downstream of the nozzle. In general, the flow is displaced around the jet and then converges back towards the centerline. The structure downstream of the nozzle is a result of a pair of contra-rotating vortices that have the common flow towards the wall (-y direction). Oil in this region is displaced away from the centerline of the wind tunnel. Numerical predictions performed at the NASA Lewis Research Center using the RPLUS[18] flow solver indicate the presence of these vortices. This feature of shallow angle injection is believed to be previously unreported.

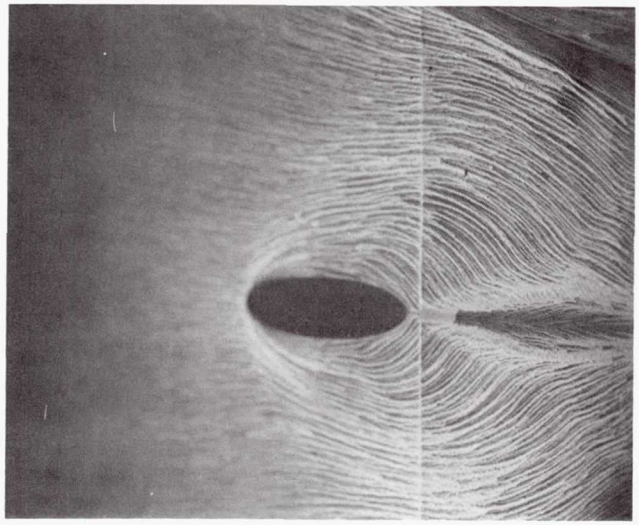

Fig. 5. Oil flow visualization for Case 8.

Mach Contours

The static and pitot pressure surveys were used to calculate Mach number distributions in the cross plane. These results are shown for the twelve operating conditions in Figs. 6a through 6l, respectively. The peak Mach number observed in the cross section is also shown in the figures. A physical limitation of the probe traversing mechanism only allowed the surveys to be extended to the z/D=-2 location. This limitation was corrected for the trace gas measurements. In general, the flowfield for all cases is characterized by the pressure induced vortex pair associated with a jet in a cross flow.[12] These vortices create the outward bulging of the contours away from the wall and are in addition to the aforementioned near wall vortex pair that were evident in the oil flow visualization (Fig. 5). Although the near wall vortices are not resolved by the transverse flowfield measurements, evidence of their presence can be seen in Figs. 6i and 6l, where the near wall contour (M=1.4) in the vicinity of z/D=0 bulge inward towards the wall. A certain degree of asymmetry is observed to be present at the lower freestream Mach numbers (Figs. 6a through 6f). A similar asymmetry was observed for the 15° sonic helium jet investigated by Mays *et al.*[7], which they attributed to the high streamwise vorticity in the flow. For Cases 8-12, the effective pressure ratio causes sufficient expansion of the jet flow, producing local regions in the measurement cross plane where the Mach number exceeds the nozzle exit Mach number. It should be noted here that for Mach numbers greater than approximately 4.5, the operating total temperature of the streams (T_t = 294° K) was not high enough to prevent condensation of the air stream. The number of Mach number peaks in the cross plane tends to increase as the freestream Mach number increases. At M_∞=1.6 and 2.0 (Figs. 6a through 6f), two peaks in the Mach number are observed which are nominally symmetric about the y-axis. For M_∞=2.5 (Figs. 6g through 6i), a third peak appears along the plane of symmetry (y-axis). For M_∞=3.0 (Figs. 6j through 6l), in addition to the peak along the y-axis, two pair symmetrically located about the y-axis are observed.

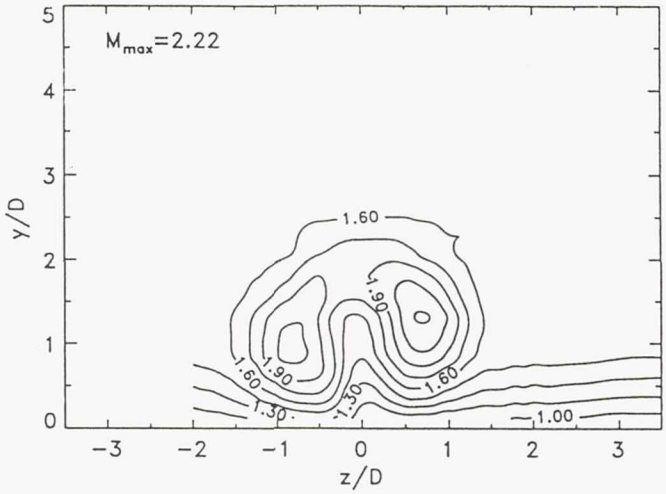

a) Case 1, M_∞=1.6, $\bar{q}$=4.10.

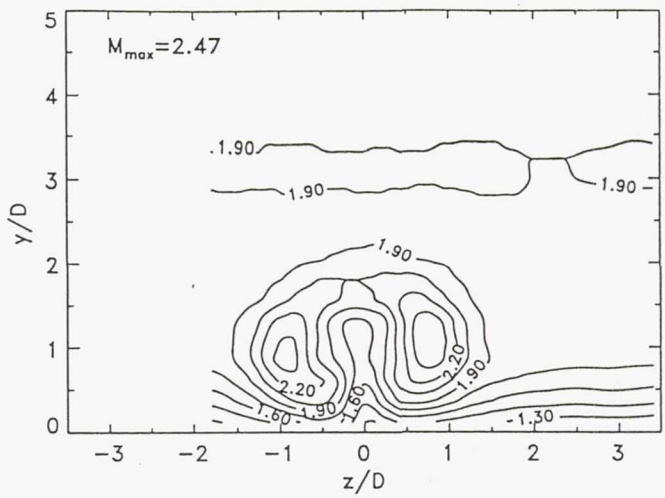

d) Case 4, M_∞=2.0, $\bar{q}$=3.14.

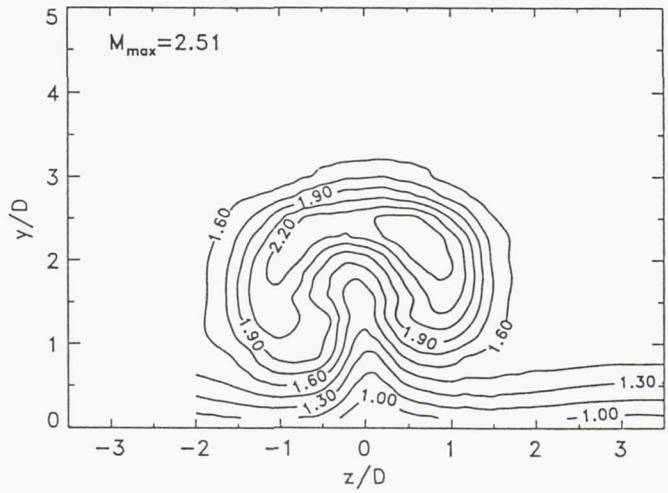

b) Case 2, M_∞=1.6, $\bar{q}$=6.15.

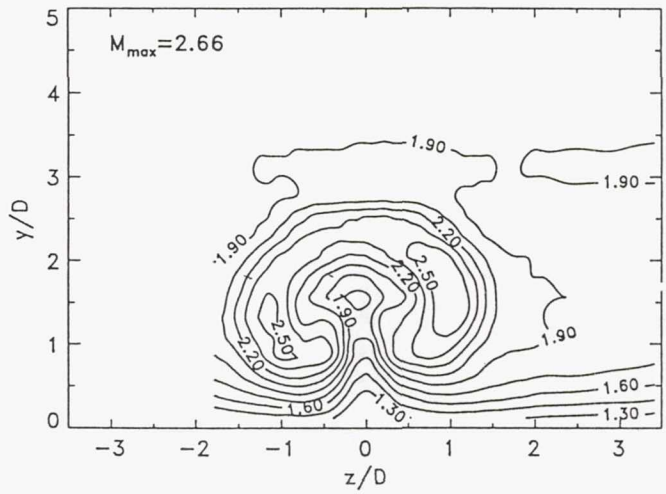

e) Case 5, M_∞=2.0, $\bar{q}$=4.71.

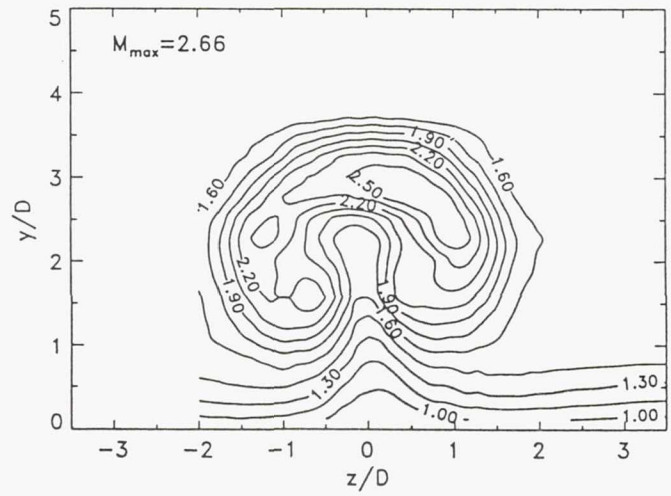

c) Case 3, M_∞=1.6, $\bar{q}$=8.20.

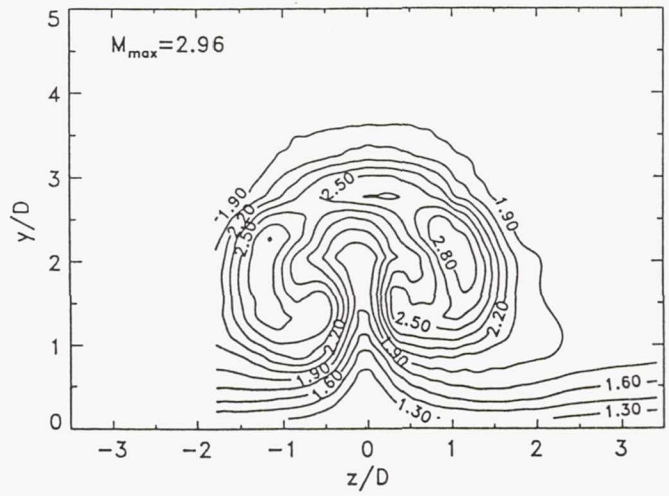

f) Case 6, M_∞=2.0, $\bar{q}$=6.28.

Fig. 6. Mach number contours at x/D=15.

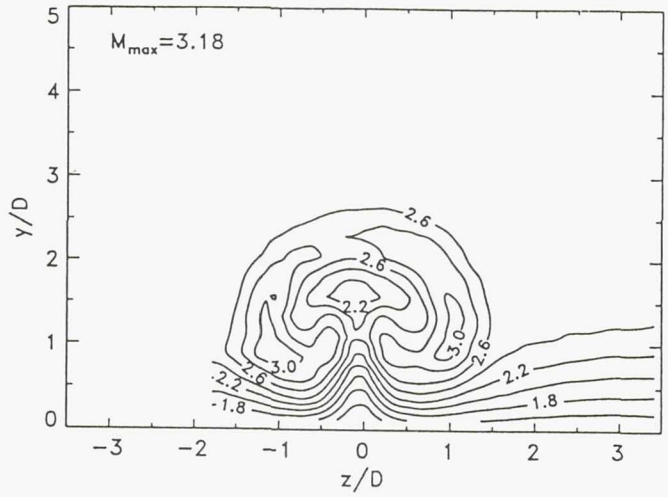

g) Case 7, M_∞=2.5, $\bar{q}$=3.51.

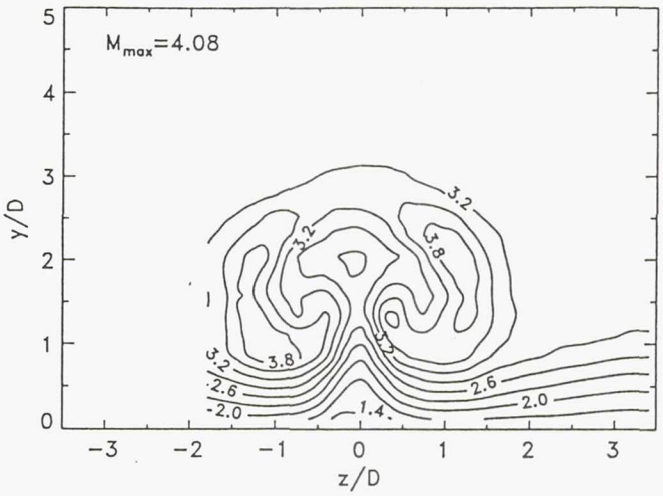

j) Case 10, M_∞=3.0, $\bar{q}$=4.37.

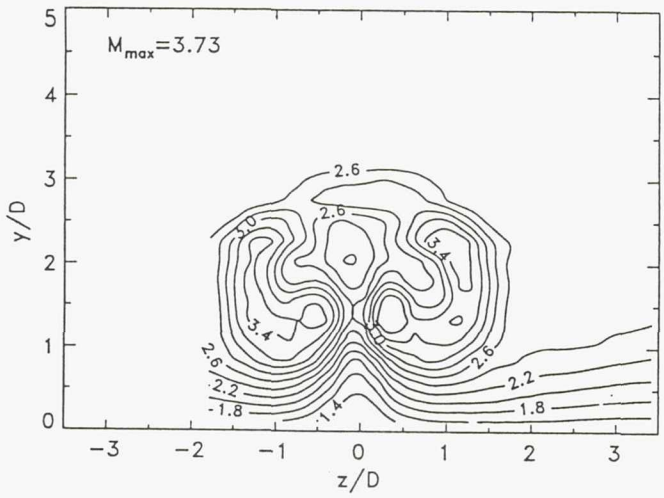

h) Case 8, M_∞=2.5, $\bar{q}$=5.27.

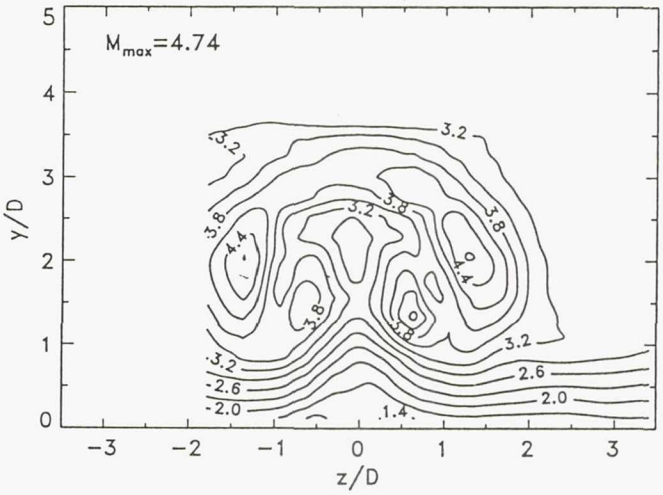

k) Case 11, M_∞=3.0, $\bar{q}$=6.55.

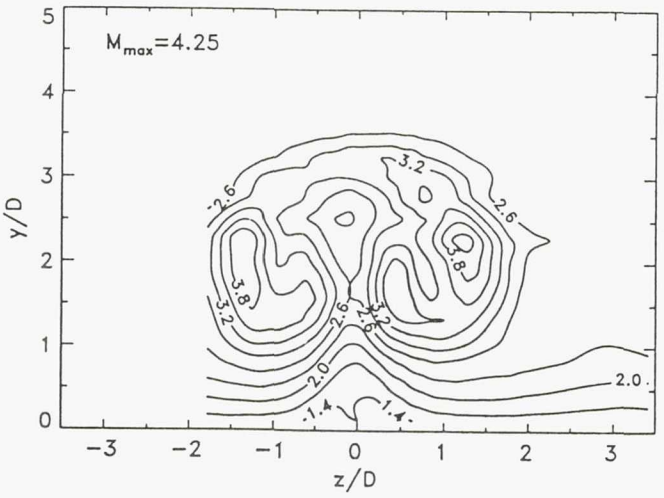

i) Case 9, M_∞=2.5, $\bar{q}$=7.03.

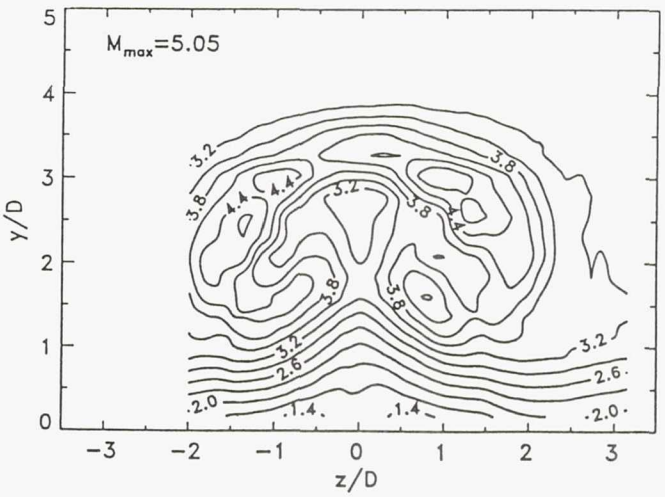

l) Case 12, M_∞=3.0, $\bar{q}$=8.74.

Fig. 6. Mach number contours at x/D=15.

Mixing Behavior

Trace gas measurements were made for Cases 3, 5, 8 and 11. Contours of the volume (mole) fraction in the measurement plane, as well as the peak concentration measured, are shown in Figs. 7a through 7d. The vortex induced pattern of the contours is similar to that observed in the Mach number contours. The asymmetry observed for the lower freestream Mach numbers is also present in the trace gas results. The spreading of the jet is observed to be largest for Case 3. A feature of this case that is not observed in the others is the outward bulging of the lowest contour level in the vicinity of y/D=1, z/D=±2. This is believed to be a result of the interaction between the reflected oblique shock and the jet stream. It is also likely that this interaction enhances mixing for this case. It is interesting to note that, with the exception of Case 3, the spreading of the jet increases as the freestream Mach number increases (M_j/M_∞ decreases), which is opposite to what would be expected with all other variables being constant.

In order to quantify the mixing between the two streams, the mixing efficiency proposed by Hollo *et al.*[17] will be used. The mixing efficiency is defined as the percentage of the test section area that is considered to be "mixed". Hollo suggests that the flow is considered mixed when the volume fraction (v) is between the static flammability limits for hydrogen in air, namely; 4 to 74%. The choice of this range is somewhat arbitrary, but is useful for comparative purposes. For the present study, the lower limit was specified as the lower flammability limit for hydrogen in air (v_L=0.04), but in order to get a better idea of the distribution of the mixture, mixing efficiencies based several upper limits are presented (v_U=0.25, 0.5, 0.74 and

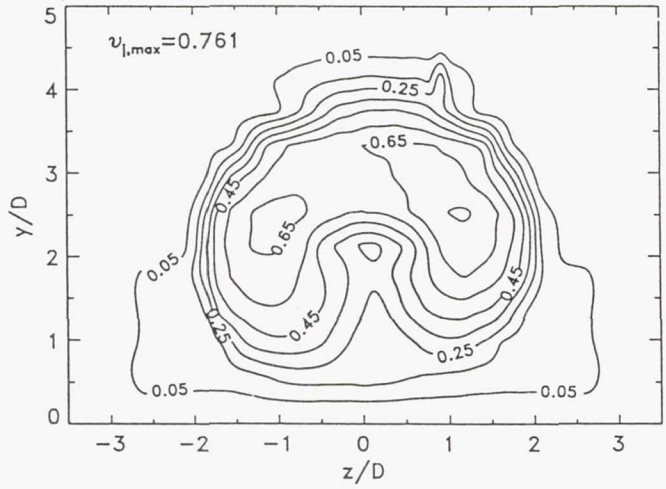

a) Case 3, M_∞=1.6, $\bar{q}$=8.20.

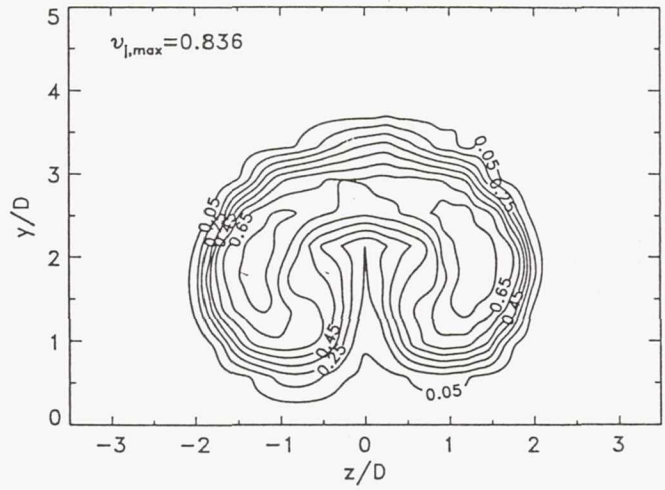

c) Case 8, M_∞=2.5, $\bar{q}$=5.27.

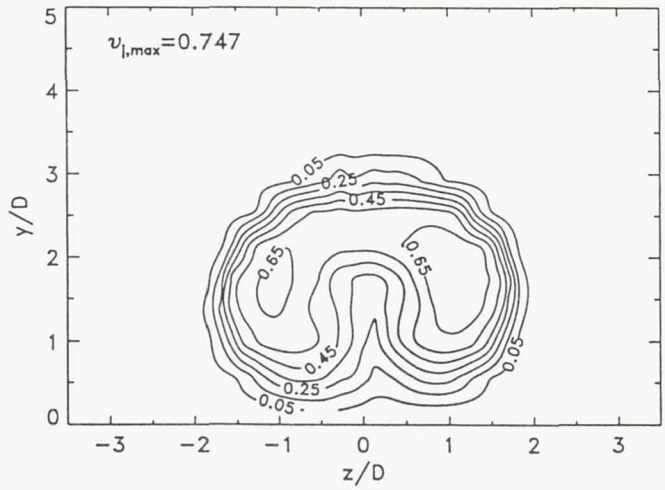

b) Case 5, M_∞=2.0, $\bar{q}$=4.71.

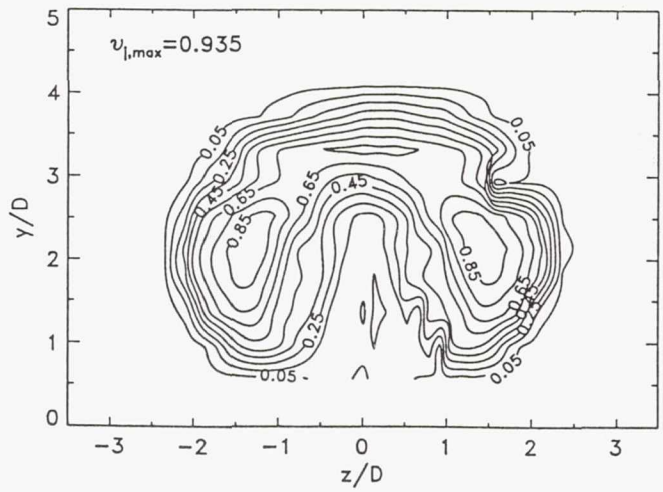

d) Case 11, M_∞=3.0, $\bar{q}$=6.55.

Fig. 7. Volume fraction contours at x/D=15.

1.0). The mixing efficiency defined in this manner is plotted against the dynamic pressure ratio in Fig. 8. The curve labeled v_U=1.0 represents the fraction of the test section area through which at least a trace ($v \geq 0.004$) of the jet fluid passes and is an indication of the degree of spreading of the jet. The curve labeled v_U=0.74 represents the fraction of the test section area that is within the static flammability limits for hydrogen in air. For Cases 3 and 5, essentially all of the mixture in the cross plane is below the upper flammability limit (see Figs. 7a and 7b). Although the data is limited, the spreading of the jet appears to correlate strongly with the dynamic pressure ratio. Another interesting feature is that the cases which had the lowest (Case 5) and highest (Case 11) peak concentration levels, also had the smallest and second largest mixing efficiencies, respectively. This implies that peak concentration is not a good indicator of overall mixing.

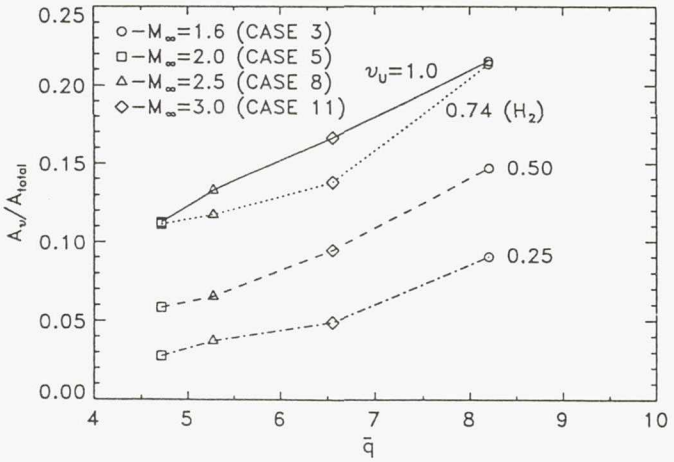

Fig. 8. Mixing efficiency vs. $\bar{q}$ at x/D=15.

Jet Penetration

For the aerodynamic measurements, the jet penetration is defined as the location along the y-axis (symmetry plane) where the Mach number is at a peak. Similarly, for the trace gas measurements, the penetration is defined as the location along the plane of symmetry where the peak concentration occurs. The penetration heights as defined above are plotted versus dynamic pressure ratio in Fig. 9. At lower values of $\bar{q}$, the location of peak concentration corresponds with the peak Mach number location, but then deviates at higher values of $\bar{q}$. The data, however, are too limited to draw any definitive conclusions. For the three lower freestream Mach numbers, the slope of the penetration curves are seen to be similar, but a decrease in sensitivity to dynamic pressure ratio is observed for the M_∞=3.0 data.

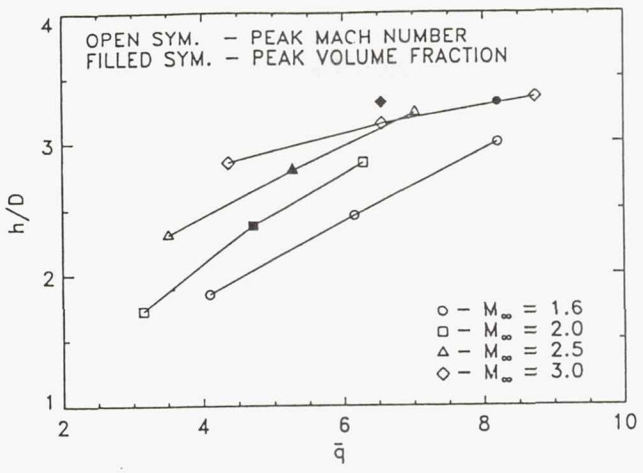

Fig. 9. Jet penetration vs. $\bar{q}$ at x/D=15.

Penetration correlations for normal sonic injection have been proposed and are reviewed by Rogers.[15] These correlatons are typically of the form:

$$h/D = a(\bar{q})^b(x/D)^c \tag{2}$$

The present data indicate a Mach number ratio dependence so that an equation of the form:

$$h/D = a(\bar{q})^b(\bar{M})^c(x/D)^d \tag{3}$$

was used to attempt to correlate the aerodynamic penetration data with dynamic pressure ratio and Mach number ratio. A least-squares curve fit of the data to this equation is shown in Fig. 10. At least over the conditions considered in the present study, this relation provides a reasonable description of the jet penetration.

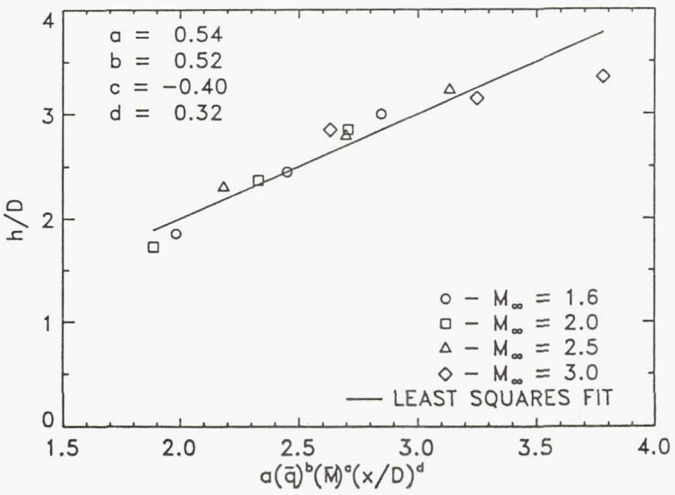

Fig. 10. Jet penetration correlation.

Concluding Remarks

Flowfield measurements in a plane 15 nozzle diameters downstream of a supersonic jet injected at a 10° angle into a supersonic stream have been presented. The experimental results, along with the supporting CFD calculations, show that the flowfield is characterized by two vortex pairs. The pair furthest from the wall significantly distorts the jet mean flowfield. The results also indicate that jet penetration and mixing correlate strongly with dynamic pressure ratio. In addition, at a given dynamic pressure ratio, the jet penetration was observed to be inversely proportional to Mach number ratio. A correlation has been presented that describes the jet penetration for the present configuration, but additional data at other axial locations is needed for verification.

The present data set can be used for CFD calibration and validation purposes, inasmuch as cross plane data is presented over a fairly wide range of operating conditions and upstream conditions are well defined. For the jet flow, calculations should begin at the throat of the nozzle since it is unlikely that the flow is uniform at the jet exit. The splitter plate, as well as the wind tunnel walls, should be modeled to account for oblique shock wave interaction in the flowfield.

References

[1]Northram, G.B., Greenburg, I. and Byington, C.S., "Evaluation of Parallel Injector Configurations for Supersonic Combustion," AIAA Paper 89-2525, 1989.

[2]Orth, R.C., Schetz, J.A. and Billig, F.S., "The Interaction and Penetration of Gaseous Jets in Supersonic Flow," NASA CR-1386, July 1969.

[3]Billig, F.S., Orth, R.C. and Lasky, M., " A Unified Analysis of Gaseous Jet Penetration," AIAA Journal, Vol.9, No.6, June 1967, pp.1048-1058.

[4]Schetz, J.A. and Billig, F.S., "Penetration of Fluid Jets into a Supersonic Stream," *J. Spacecraft and Rockets*, Vol.3, No.11, Nov. 1966, pp.1658-1665.

[5]Schetz, J.A., Hawkins, P.F. and Lehman, H., "Structure of a Highly Underexpanded Transverse Jets in a Supersonic Stream," *AIAA Journal*, Vol.5, No.5, May 1967, pp.882-884.

[6]Schetz, J.A., Weinraub, R.A. and Mahaffey, R.E., "Supersonic Transverse Injection into a Supersonic Stream," *AIAA Journal*, Vol.6, May 1986, pp.933-934.

[7]Mays, R.B., Thomas, R.H. and Schetz, J.A., "Low Angle Injection Into a Supersonic Flow," AIAA Paper No. 89-2461, 1989.

[8]Zukoski, E.E. and Spaid, F.W., "Secondary Injection of Gases into a Supersonic Stream," *AIAA Journal*, Vol.2, No.10, Oct. 1964, pp.1689-1696.

[9]Cohen, L.S., Coulter, L.J. and Egan, W.J., Jr., "Penetration and Mixing of Multiple Gas Jets Subjected to a Cross Flow," *AIAA Journal*, Vol.9, No.4, April 1971, pp.718-724.

[10]Koch, L.N. and Collins, D.J., "Variations in Secondary Mach Number and Injection Angle in Jet Interaction," *AIAA Journal*, Vol.9, No.6, June 1971, pp.1214-1215.

[11]Lee, R.E and Linevsky, M.J., "Shadowgraph Studies of Angular Injection of a Sonic Jet into a Mach 2.8 Supersonic Flow," AIAA Paper 90-1618, 1990.

[12]Fearn, R. and Weston, R.P., "Vorticity Associated with a Jet in a Cross Flow," *AIAA Journal*, Vol.12, No.12, Dec. 1974, pp.1666-1671.

[13]Faucher, J.E., Goldstein, S. and Tabach, E., "Supersonic Combustion of Fuels Other Than Hydrogen for Scramjet Application," AFAPL-TR-67-12, U.S. Air Force, Feb. 1967.

[14]McClinton, C.R., "The Effect of Injection Angle on the Interaction Between Sonic Secondary Jets and a Supersonic Freestream," NASA TN D-6669, Feb. 1972.

[15]Rogers, R.C., "A Study of the Mixing of Hydrogen Injected Normal to a Supersonic Stream," NASA TN D-6114, March 1971.

[16]Rogers, R.C., "Mixing of Hydrogen Injected from Multiple Injectors Normal to a Supersonic Stream," NASA TN D-6476, Sept. 1971.

[17]Hollo, S.D., Hartfield, R.J. and McDaniel, J.C., "Injectant Mole Fraction Measurements of Transverse Injection in Constant Area Supersonic Ducts," AIAA Paper 90-1632, 1990.

[18]Yu, S., Tsai, Y.P. and Shuen, J., "Three-Dimensional Calculation of Supersonic Reacting Flows Using an LU Scheme," AIAA Paper 89-0391, 1989.

NASA
National Aeronautics and Space Administration

Report Documentation Page

1. Report No.	2. Government Accession No.	3. Recipient's Catalog No.
NASA TM-103726 AIAA-90-5240		

4. Title and Subtitle

Experimental Investigation of a Single Flush-Mounted Hypermixing Nozzle

5. Report Date

6. Performing Organization Code

7. Author(s)

David O. Davis, Warren R. Hingst, and A. Robert Porro

8. Performing Organization Report No.

E-5960

10. Work Unit No.

505-62-31

9. Performing Organization Name and Address

National Aeronautics and Space Administration
Lewis Research Center
Cleveland, Ohio 44135-3191

11. Contract or Grant No.

13. Type of Report and Period Covered

Technical Memorandum

12. Sponsoring Agency Name and Address

National Aeronautics and Space Administration
Washington, D.C. 20546-0001

14. Sponsoring Agency Code

15. Supplementary Notes

Prepared for the Second International Aerospace Planes Conference , sponsored by the American Institute of Aeronautics and Astronautics, Orlando, Florida, October 29-31, 1990. Responsible person, David O. Davis, (216) 433-8116.

16. Abstract

Reported herein are the results of an experimental wind tunnel investigation of a circular supersonic jet ($m_j = 3.47$) injected at a 10 degree angle into a supersonic freestream. The jet penetrates a boundary layer, which has a thickness approximately the same as the jet nozzle exit diameter. Measurements were made for nominal freestream Mach numbers of 1.6, 2.0, 2.5 and 3.0. Three jet total pressures were run at each freestream Mach number, resulting in twelve separate operating conditions. Mean data accumulated by means of static and total pressure probe instrumentation are presented at two axial stations: seven jet nozzle diameters upstream and 15 jet nozzle diameters downstream from where the centerline of the nozzle intersects the wind tunnel wall. For one condition at each freestream Mach number, the jet air was seeded with a hydrocarbon trace gas and the flow was sampled at the downstream measurement plane to quantify the mean mixing of the two streams. Surface oil flow visualization was also used to investigate the flow interaction. All results are for air-to-air mixing. The measurements indicate the presence of two pairs contra-rotating vortices. One pair follows the jet trajectory and tends to split the jet into two streams. A smaller pair, rotating in an opposite sense, develops in the near wall region. Reported results include Mach number and volume fraction distributions in the cross plane, as well as jet penetration and mixing efficiency.

17. Key Words (Suggested by Author(s))	18. Distribution Statement
Hypermixing nozzle Supersonic jets	Unclassified – Unlimited Subject Categories 02 and 34

19. Security Classif. (of this report)	20. Security Classif. (of this page)	21. No. of pages	22. Price*
Unclassified	Unclassified	12	A03

*For sale by the National Technical Information Service, Springfield, Virginia 22161